Surface plasmon polariton in multilayered configuration

R. Ahmed Ammar[1-*], *M. Lemerini*[1]

[1]Laboratory of Theoretical Physics, Department of Physics, Faculty of Sciences, University of Abou Bekr Belkaid, B. P 119, 13000, Tlemcen, Algeria
*) Email: ri.ahmedammar@gmail.com

Received 14/10/2018, *Accepted* 28/5/2019, *Published* 15/9/2019

We investigate the effect of a propagation of surface electromagnetic waves along a metallic surface covered by layered dielectric structures. The optical coupling of a wave incident to collective oscillations of electrons along an interface between a metal and a dielectric is governed by the thickness of metal and gap layers. The surface Plasmon excited by an electromagnetic wave with a central wavelength of λ=486 nm and using the optic finite-difference time-domain method (OptiFDTD). For the metal, in particular a frequency on their dielectric permittivity dependence and described by the Drude-Lorentz model and using the effective-index approach and an explicit expression for the propagation constant of long rang surface plasmon polaritons (LR-SPPs) obtained for moderate metal widths.

Keywords: EMW; Metallic; Optical.

1. INTRODUCTION

Surface plasmon polaritons (SPPs) are waves trapped on the surfaces of metals owing to the interaction between the free electrons in a metal and the electromagnetic field in a dielectric. This application note demonstrates the concept of multi-channel wavelength filtering using a nanophotonic structure that is based on a metal-insulator-metal (MIM) and insulator-metal-insulator (IMI) plasmonic waveguide structure with a nanodisk resonator **[1, 2]** The TM polarized SP mode is uniquely characterized by its magnetic field lying in the plane of the metal-insulator surface and perpendicular to the wave propagation direction. The metal commonly used to excite surface plasmon polaritons (SPPs) is silver (Ag) due to their remarkable optical properties described by the frequency dependent complex permittivity $\varepsilon_m(\omega) = \varepsilon_m^r(\omega) + i\,\varepsilon_m^i(\omega)$ in the

Exp. Theo. NANOTECHNOLOGY 3 (2019) 395-404
Drude-Lorentz model($\varepsilon_m^r < 0,\ |\varepsilon_m^r| \gg \varepsilon_m^i$). Since the SPR is the resonance phenomenon corresponding to an energetic transfer from incident light to SPPs. Liquid crystals combine the physical and optical properties of both liquids and solids. The E7 **[3, 4], [15]**, nematic liquid crystals mixture contains cyanobiphenyl and cyanoterphenol components, at a specific composition, which possess relatively high birefringence and positive dielectric anisotropy. Due to these properties, it is widely used in polymer dispersed liquid crystals **[5], [16]**. The specific composition is critical to ensure physical properties and characteristic of the liquid crystal. The specific composition is critical to ensure physical properties and characteristic of the liquid crystal. Even small changes can have pronounced effects on factors such as the nematic to isotropic transition, and glass transition temperatures. E7 is used as the dielectric ε_d in the temperature $25\ c^0$ on IMI configureuration.

2. THE DRUDE-LORENTZ MODEL

The Lorentz model (1905) is a refining of the Drude model, in which the statistical aspects are specified. The electrons are considered as free charges, with charge "-e"; they are described by a maxwellian velocity distribution. Considering an electron gas in a spatial region with a constant electric field, the drift velocity of the electrons is constant; this corresponds to a current density $\vec{j}$ proportional to the applied field $\vec{j} = \sigma_0 \vec{E}$, with 2 σ0 =ne τ /m (n is the electron density). Estimating the relaxation time τ, Drude and Lorentz have obtained values of conductivity in good accordance with the experiments. In presence of an electric field of the form E(t)=E0 $e^{-i\omega t}$, the complex conductivity assumes the form $\sigma\omega = \sigma_0 / (1 - i\omega\tau)$. Such model, said "Drude-Lorentz model", has received great success, but has also underlined series difficulties. The Drude-Lorentz model often used for parameterization of the optical constants of metals. A complex dielectric function for some metals and surface plasmas can be expressed in the following form:

$$\varepsilon_{DL}(\omega) = \varepsilon_D(\omega) + \varepsilon_L(\omega) \quad (\mathbf{1})$$

This model has two terms: the Drude term $\varepsilon_D(\omega)$ for the free-electron resonance. The intraband transition of electrons from filled bands to the conduction band can significantly influence the optical response, and it can describe the transport properties of electrons in good conductors, and the the Lorentz term $\varepsilon_L(\omega)$, takes the interband effects into the account for simulations, and the bound electrons are described by forced and damped harmonic oscillators. The relative dielectric function is [6], [13], [16] :

Exp. Theo. NANOTECHNOLOGY 3 (2019) 395-404

$$\varepsilon_{DL}(\omega) = 1 - \frac{f_0 \omega_p^2}{\omega^2 - i\,\omega\,\Gamma_0} + \sum_{j=1}^{k} \frac{f_j\,\omega_p^2}{\Omega_j^2 - \omega^2 + i\,\omega\Gamma_j} \qquad (2)$$

Where w_P is the plasma frequency, k is the number of oscillators with frequency Ω_j, strength f_j, and life time $1/\Gamma_j$.

Table 1 Optimized parameters of the Drude–Lorentz model for Silver metal. **[6]**, ω_p, Ω_j and Γ_j are in electron volts, f_j has no units.

$\omega_p = 9.01$	$f_2 = 0.124$	$f_4 = 0.840$
$f_0 = 0.845$	$\Gamma_2 = 0.452$	$\Gamma_4 = 0.916$
$\Gamma_0 = 0.0\ 48$	$\Omega_2 = 4.481$	$\Omega_4 = 9.083$
$f_1 = 0.065$	$f_3 = 0.011$	$f_5 = 5.646$
$\Gamma_1 = 3.886$	$\Gamma_3 = 0.065$	$\Gamma_5 = 2.419$
$\Omega_1 = 0.816$	$\Omega_3 = 8.185$	$\Omega_5 = 20.29$

In Figure. 1 we have plotted the real and imaginary parts of the dielectric function of silver as tabulated in **[6]**, as well as the description achieved using the DL model.

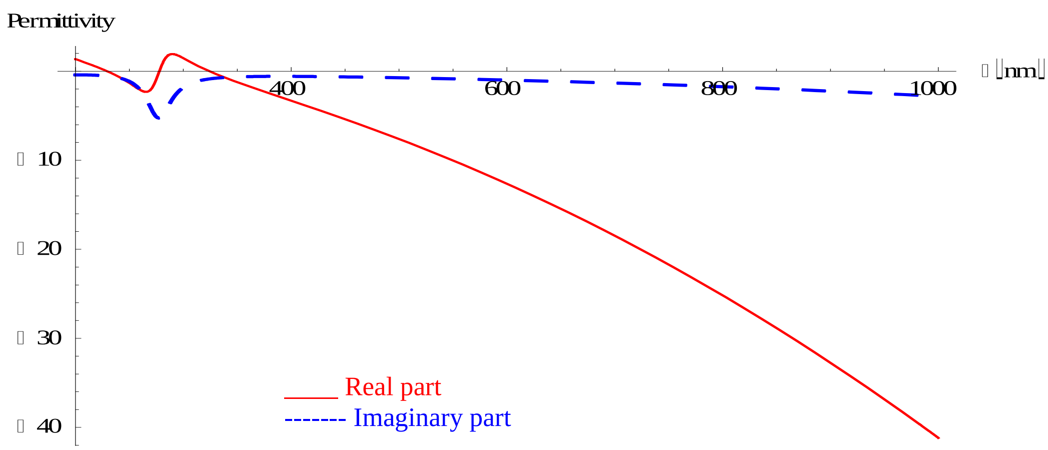

Figure 1 Tabulated silver dielectric function with the D-L model, Real part and Imaginary part.

Exp. Theo. NANOTECHNOLOGY 3 (2019) 395-404

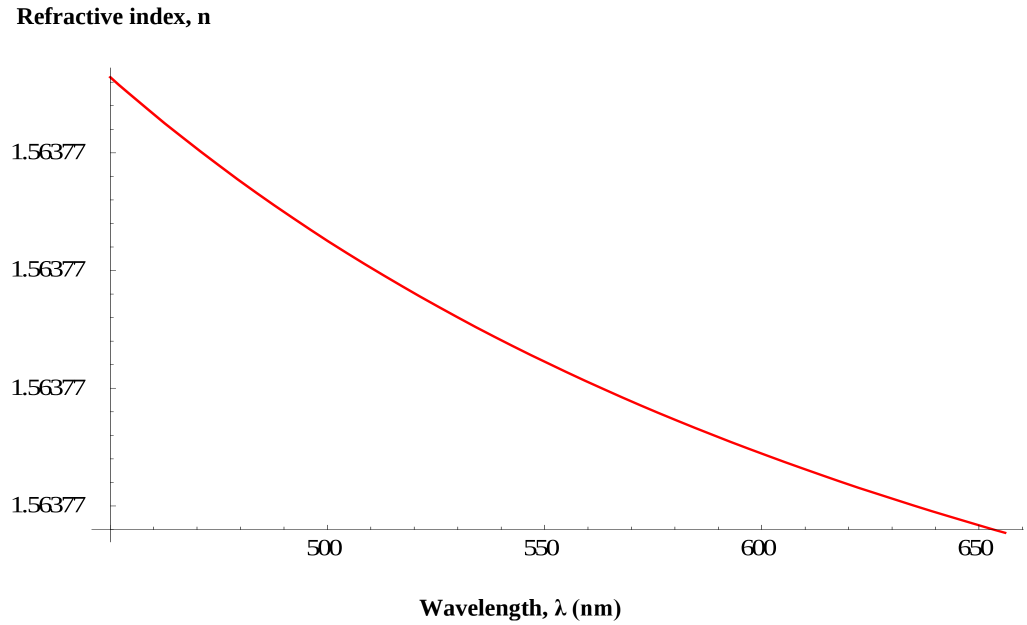

Figure 2 The refractive index of the liquid crystal (E7) as a function of wavelength between 450-656 nm **[3]**.

Figure 2 shows the refractive index of E7 as a function of wavelength between 486 nm, We consider the dielectric is the E7 nematic liquid crystal at T=25 c° wich the complex dielectric function ε_d and the complex index of refraction $\hat{n}$ are defined as **[13]** :

$$\varepsilon_d = \varepsilon_1 + i\,\varepsilon_2 = \hat{n}^2 = (n + i\,k)^2 \quad (3)$$

$$\hat{n} = n + i\,0 = n = \frac{ne+2*n0}{3}$$

For λ=486 nm, ne=1.8005, n0=1.5424.

n= 1.61563

$$\varepsilon_d = \varepsilon_1 = n^2 = 2.61026$$

3. SURFACE PLASMONS IN IMI-STRUCTURE (METAL FILM)

An important extension of the simple metal surface is a three-layer system sometimes also called heterostructure [7], where each of the layers has an infinite extension in two dimensions. Two basic heterostructures can be distinguished, a dielectric gap in a metal, or MIM (metal-insulator-metal) system [17] and a metal film surrounded by two dielectrics, or IMI (insulator-metal-insulator) system [12]. A metal film bounded by two dielectric materials is also known as IMI structure [10]. In 1969, Economou [11] conducted the first systematic study of SP's on single as well as multilayer metal films surrounded by symmetric dielectrics(E7). In this section we consider the SPP modes in the symmetric IMI configureuration of a thin metal film with the thickness w being embedded in the dielectric. The symmetric transverse field configureuration is called the symmetric SPP mode. Since the SPP damping is determined by the longitudinal SPP component, the symmetric SPP mode exhibiting the odd symmetry of longitudinal field (which thereby crosses zero changing its sign) at the mid-plane of the metal film experiences considerably smaller attenuation. We consider here a slab of a medium with permit-tivity ε_{Ag} and width w. For sufficiently small metal widths (w→ 0), one can use the approximation tanh(x) ≈ x resulting the dispersion relation for the metal (Ag) can be written for the symmetric field distribution as **[1, 8]** :

$$\tanh\left(k_z^{(m)}\ \frac{w}{2}\right) = -\frac{\varepsilon_m\, k_z^{(d)}}{\varepsilon_d\, k_z^{(m)}} \qquad \text{with} \qquad k_z^{(m,d)} = \sqrt{\beta^2 - \varepsilon_{m,d}\, k_0^2} \tag{4}$$

$$\beta \approx k_0 \sqrt{\varepsilon_d + \left(\frac{k_0\, \varepsilon_d\, w}{2}\right)^2 + \left(1 - \frac{\varepsilon_d}{\varepsilon_m}\right)^2} \tag{5}$$

Where β denotes the propagation constant of the fundamental gap surface plasmons polariton (GSPP) mode with the transverse field component E_z having the same sign across the gap, $\varepsilon_{m,d}$ the permttivities of metal and insulator (E7).with $k_0 = \frac{2\pi}{\lambda}$ Here, k_0 is the wave vector of incident light, λ is the wavelength. The imaginary part of the propagation constant is associated with the attenuation and propagation lenght of the surface plasmon in the direction of propagation. The propagation constant is related to the effective index n_{eff} , propagation length L and attenuation b **[2], [9]** as

$$n_{eff} = \frac{\mathrm{Re}(\beta)}{k_0}$$
$$L = \frac{1}{2\,\mathrm{Im}(\beta)} \tag{6}$$
$$b = \frac{0.2}{\ln(10)}\ \mathrm{Im}(\beta)$$

where Re{} and Im{} denote the real and imaginary parts of a complex number, respectively; the attenuation b is in dBcm^{-1} if β is given in m^{-1}.

Exp. Theo. NANOTECHNOLOGY 3 (2019) 395-404

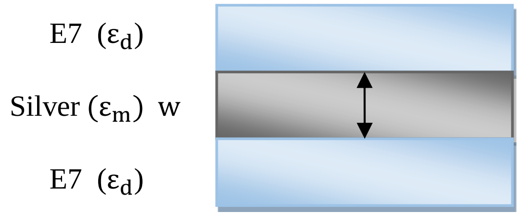

Figure.3. Schematic of IMI plasmonic waveguide.

The inset in figure 3 shows the IMI geometry a thin metallic film (Ag) of thickness 2w sandwiched between two insulating layers (E7). In this case ε_m represents the dielectric function of the metal, and ε_d the positive, real dielectric constant of the insulating sub- and superstrates.

4. RESULTS AND DISCUSSION

Figure 4 shows that the effective index, propagation length and attenuation of SPP mode change with width for a silver film. The effective index, propagation length and attenuation could be acquired by numerically solving Eq. (3). The symmetric surface plasmon exhibits effective index and attenuation, which increase with an increasing metal film width, and propagation length decreases with an increasing metal film width.

a) b)

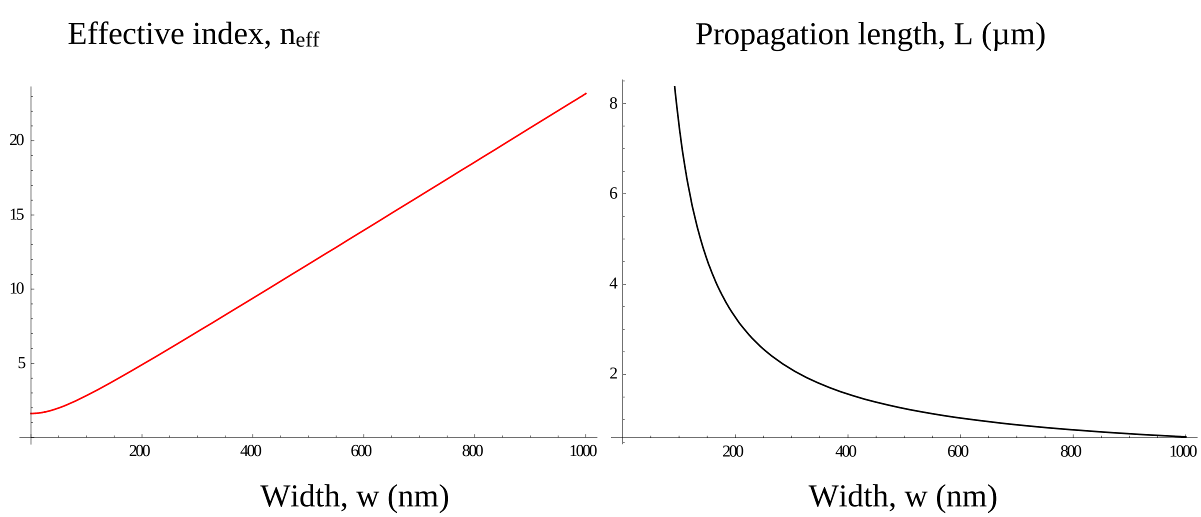

Attenuation, b (dB cm^{-1})
$\times 10^5$

c)

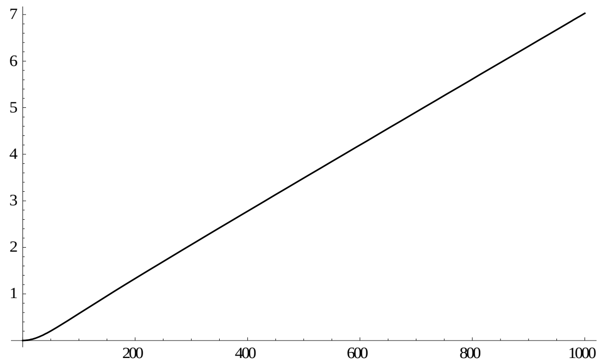

Figure 4 Description of MIM plasmonic waveguides (E7/Ag/E7, $\varepsilon_d = 2.61026$ and silver metal ε_{Ag} = - 6.97534 – i*0.70002 and wavelength λ=486 nm) as a function of width of the silver metal by (a) effective index, (b) propagation length and (c) the attenuation.

Figure 4 shows that the effective index, propagation length and attenuation of SPP mode change with width for a silver film. The effective index, propagation length and attenuation could be acquired by numerically solving Eq. (3). The symmetric surface plasmon exhibits effective index and attenuation, which increase with an increasing metal film width, and propagation length dencreases with an increasing metal film width.

We use software of OptiFDTD **[14]** to calculate Transverse magnetic field and Transmission spectrum. In figure 5 shows (a) the magnetic field profile is presented in the plane (x, z) for λ=486 nm (in vacuum) and for a symmetric IMI configureuration with permitivities $\varepsilon_d = 2.61026$ and $\varepsilon_{Ag} = -6.97534 - i * 0.70002$. Thus, the transverse magnetic field Hy(x), which is continuous at the interface and (b) we present the calculated transmission spectrum spectra as a function of the wavelength with length l = 100 nm and metal width w = 50 nm.

a)

b)

Exp. Theo. NANOTECHNOLOGY 3 (2019) 395-404

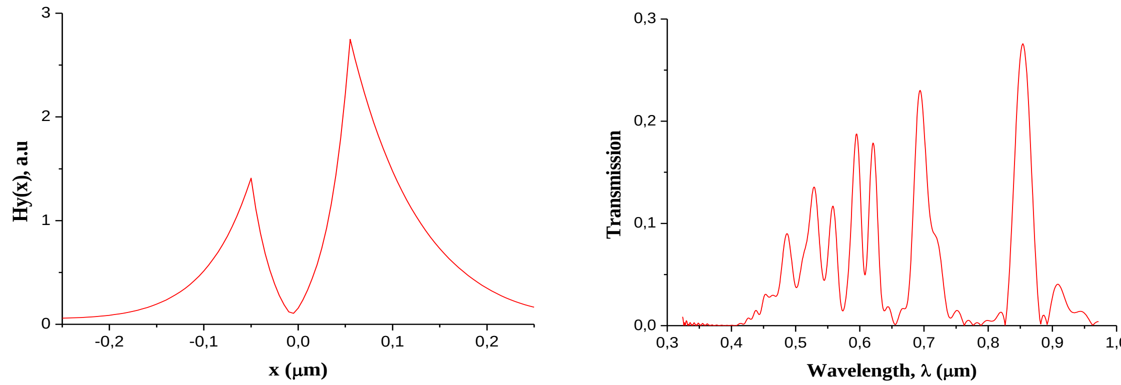

Figure 5 (a) Surface plasmon magnetic field profile of E7-silver-E7 guide (λ_0 = 633nm, 2w = 0.1 μm) and (b) the transmission spectrum.

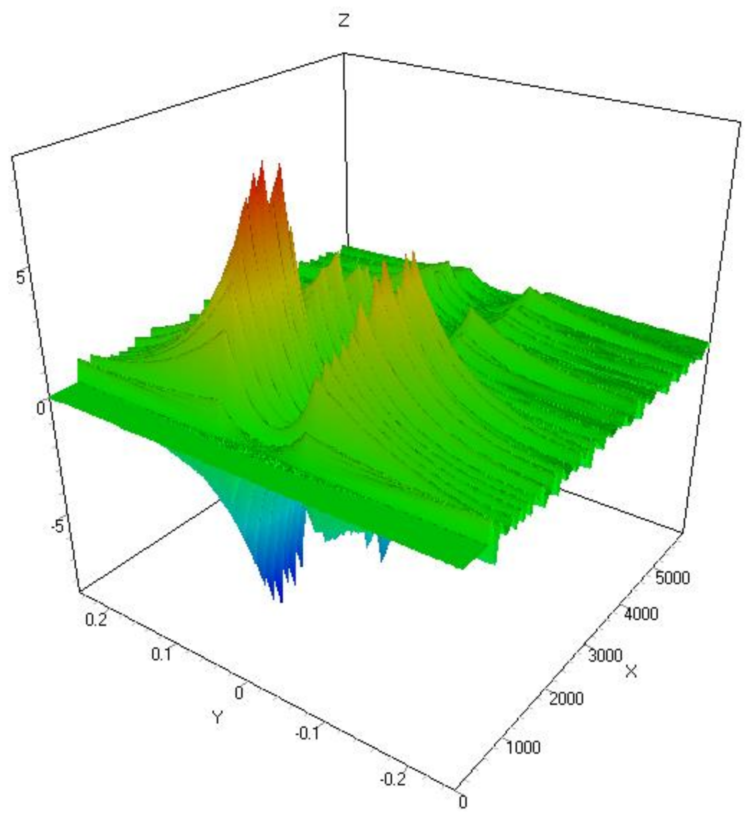

Figure 6 Geometry and charachteristic tangential magnetic field profile H_y for the seme-infinite IMI wave guide core metal thickness w. The propagate alond the positive Z direction.

Figureure 6 shows the SPP dispersion curves for E7-Ag-E7 IMI structures with various silver layer thickness are film thickness. The IMI symmetric mode exhibits a cut-off for core films.

5. CONCLUSIONS

We analyzed propagation of surface plasmon polariton (SPP) through various layered structures in which the metallic surface is covered by strips of dielectric materials with different dielectric permittivity. we use a insulator-metal-insulator (IMI) structure to generate plasmon surface polaritons. In a first step, we study the influence of the metal thickness on the resonance SPP. In a second step, we present the analytical results of the effective index, attenuation and propagation length as a function of wavelength for disposal which are excited by an electromagnetic wave in the visible band (λ=486 nm). For metal, we took a particular frequency dependence on their dielectric permittivity $\varepsilon_{Ag}(\lambda)$ and are tabulated in the reference **[6]**. We finally find the basic characteristics for SPP.

References

[1] Z Han and S I Bozhevolnyi, Rep. Prog. Phys. 76 (2013) 016402

[2] Jiri Homola, Springer Ser Chem Sens Biosens 4 (2006) 3

[3] N. Geetha, S. Sivaranjani, A. Ayeshamariam, Mariadhas Valan Arasu, N. Punithavelan, Exp. Theo. NANOTECHNOLOGY 2 (2018) 139

[4] J Li, S Gauzia, S T Wu, optics express 12 (2004) 2002

[5] L Bedjaoui, N Gogibus, B Ewen, T Pakulab, X Coqueretc, M Benmounaa, U Maschkec, Polymer. (2004) 45: 6555

[6] A. D. Rakic´, A. B. Djurisic, J. M. Elazar, and M. L. Majewski, Applied Optics, 37 (1998) 5271

[7] B Prade, J.Y. Vinet, A. Mysyrowicz, Phys. Rev. B, 44 (1991) 13556

[8] S. I. Bozhevolnyi and T. Søndergaard, ‘’ General properties of slow-plasmon resonant nanostructures : nano-antennas and resonators, Optics express 15 (2007) 10869

[9] Jiri Homola, Chem. Rev, 108 (2008) 462

[10] S. A. MAIER, ‘’ fundamentals and applications,’’ (2007) Springer Science.

[11] E.N. Economou, Phys. Rev. 182 (1969), 539

[12] R. Zia, M.D. Selker, P.B. Catrysse, M.L. and Brongersma, J. Opt. Soc. Am. A, 21(2004), 2442

[13] M. A. Ordal, L. L. Long, R. J. Bell, S. E. Bell, R. R. Bell, R. W. Alexander, Jr., and C. A. Ward, Applied Optics, 22 (1983) 1099

[14] http://optiwave.com/

[15] J Cooper, Waters Corporation, (2013), Manchester, UK

[16] Paolo Di Sia, "Plasmonics - Principles and Applications, chapter 1, Modelling at Nanoscale, "book edited by Ki Young Kim, ISBN 978-953-51-0797-2, (2012).

[17] R. Ahmed Ammar, and M. Lemerini, Int. J. Nanoelectronics and Materials 10 (2017) 185-194

Exp. Theo. NANOTECHNOLOGY 3 (2019) 395-404